

Ozone pollution may limit the benefits of irrigation to wheat productivity in India

Gabriella Everett¹, Øivind Hodnebrog², Madhoolika Agrawal³, Durgesh Singh Yadav⁴, Connie O'Neill⁵, Chubamenla Jamir⁶, Jo Cook¹, Pritha Pande¹, Lisa Emberson^{1*}

¹Department of Environment and Geography, University of York, York, UK- YO10 5DD.

²CICERO Center for International Climate Research – Oslo, 0318, Oslo, Norway

³Department of Botany, Institute of Science, Banaras Hindu University, Varanasi 221005, India.

⁴Department of Botany, Government Raza P.G. College, Rampur, U.P. 244901, India.

⁵Stockholm Environment Institute, University of York, York, UK- YO10 5DD.

⁶Climate Studies and Knowledge Solutions Centre, Kohima, Nagaland, India.

Correspondence to: Lisa Emberson (l.emberson@york.ac.uk)

Abstract. Ground level ozone (O₃) pollution, heat and water stress are recognised as key abiotic stresses which threaten the ability of wheat yields to meet the growing demand for food production in India. The magnitude and interplay of O₃ and water-stress effects are tightly coupled via stomatal conductance and the transpiration pathway. Existing modelling methods that assess stress response as a function of O₃- and water vapour-stomatal flux are applied to assess O₃'s role in limiting productivity afforded by irrigation. We investigate the effect of these stresses on grain yield of older (HUW-234) vs recently released (HD-3118) Indian wheat cultivars under ~~recent past~~ ~~current~~ and future climates and O₃ precursor emission profiles (using RCP4.5 and RCP8.5 scenarios). Water-stress in rainfed conditions was modelled to analyse the trade-off between O₃-induced vs. water-stress-induced yield loss to quantify the extent to which water-stress mitigates O₃ stress via reduced stomatal conductance. Under rainfed conditions for the years 1996-2005, the mean water-stress-induced and O₃-induced yield loss for HUW-234 was 13.3% and 0.6% respectively. The latter was a significant decrease from the mean O₃-induced yield loss of 10.6% modelled under irrigated conditions (i.e. no water stress). Similarly, under RCP4.5 and RCP8.5 scenarios for the mid-century, water-stress induced yield losses under rainfed conditions were 10.1% and 20.0%, while mean O₃-induced yield losses were only 1.0% and 0.1% respectively. Under irrigation, O₃-induced yield losses increased to 18.5% and 13.7%, suggesting that O₃ stress will negate the beneficial effects of irrigation. The cultivar HD-3118 suffered on average 0.2% greater O₃ relative yield loss (O₃-RYL) than HUW-234 across all scenarios. The O₃-RYL increased with climate change under the RCP4.5 scenario by 7.9% and RCP8.5 by 3.0% compared to the ~~recent past~~ ~~current~~ climate. Together these findings suggest that O₃ may continue to substantially limit the productivity benefits of the use of modern cultivars bred for high gas exchange grown under irrigated conditions in India.

1 Introduction

Wheat is a vital crop for India's economy and food security; India is the second largest wheat producer in the world and most of its population gains >50% of their calorific intake from this staple grain (Tripathi and Mishra, 2017). With India's population of 1.4 billion growing at a rate of 2.23% per year (UNDESA, 2022), wheat will play a major role in ensuring food supply meets the growing demand (Tripathi and Mishra, 2017). However, India's croplands are exposed to particularly high O₃ concentrations ([O₃]) with hotspots occurring across the Indo-Gangetic Plains (IGP) (Roy et al., 2008). The 8-hour daily mean O₃ concentrations often reach up to 100 ppb in hotspots during the Rabi crop growing season (October to April) and are therefore a significant threat to India's wheat productivity (Roy et al., 2009). Currently, there are no air quality standards in India to protect crops from surface O₃, and emissions of O₃ precursors are forecast to continue to rise well into the 21st century, driven by persistent growth in industries, including mining and petroleum industries, vehicular traffic and agricultural activities (Ghude et al., 2014; Sharma et al., 2019; Yadav et al., 2019). Ozone distribution varies spatially and temporally but the IGP often experiences high levels due to the long-distance transport of O₃ and its precursors from urban, industrial or power generation centres located across northern India (Singh and Agrawal, 2017).

Ozone damages crops when it diffuses into the intracellular airspace of the leaf via the stomata which triggers a cascade of metabolic and physiological responses resulting in reduced carbon assimilation, premature leaf senescence and visible injury. Together, these effects can lead to reductions in overall yield and quality (Emberson et al., 2018). Since O₃ damage relies on stomatal O₃ flux (i.e., O₃ dose), the scale of damage caused by ambient [O₃] varies with stomatal conductance. Stomatal conductance is determined in the short-term, by environmental factors that trigger the closure of the stomata, and in the long term, by adaptations to climate change i.e., reduced stomatal density (Emberson et al., 2018). Two other factors also influence a crop's vulnerability to O₃ dose; its detoxification ability and the signal transduction pathway, which regulates the response of cells to the increased oxidative load caused by O₃ (Ainsworth et al., 2008; Kangasjärvi et al., 2005).

It is widely acknowledged that stress conditions including elevated levels of carbon dioxide (CO₂), heat and water vapour pressure deficit (VPD) and soil water deficit (all of which may be associated with climate change) decrease stomatal conductance, thus reducing O₃ flux in wheat and potentially ameliorating O₃ damage to the photosynthetic apparatus (Feng et al., 2008). In addition, several studies have found modern cultivars are more O₃-sensitive due to selection for enhanced gas exchange, which could counteract their natural adaptation of lower stomatal conductance resulting from the changing climate. Pleijel et al. (2006) and Yadav et al. (2020) observed greater O₃-related yield loss in a modern wheat cultivar, HD-3118, bred for a higher yield than HUW-234, which was attributed to the cultivar's higher stomatal density and conductance. Climate change is expected to increase the use of drought-resistant cultivars which can maintain higher stomatal conductance under drought conditions, this will likely increase crop sensitivity to O₃ (Emberson et al., 2018). Eliminating the use of cultivars with higher stomatal conductance is unlikely to improve productivity because, on a broader scale, yield losses due to water stress outweigh those from O₃ (Emberson et al., 2018). However, in major wheat-producing states like Uttar Pradesh, where irrigation is widespread (Zaveri and Lobell, 2019) yield losses due to O₃ may outweigh those due to water stress, hence the use of

cultivars with a lower stomatal conductance may be beneficial. However, eliminating this adaptation is unlikely to improve productivity because yield losses due to water stress out-weigh yield losses due to O₃ (Emberson et al., 2018) and major wheat-producing states in India such as Uttar Pradesh, are in any case, almost fully irrigated (Zaveri and Lobell, 2019).

Khan and Soja (2003) found that well-irrigated wheat plants (i.e. with a 75% soil water capacity (SWC)) suffered grain yield losses of up to 39% when exposed to accumulated O₃ concentrations over a threshold of 40 ppb (AOT40) of ~25ppm/h. Under severe moisture deficit (35% SWC), no O₃-related yield loss was observed as O₃ uptake was reduced by up to 90%. However, the grain yield of water-stressed wheat was significantly less than well-watered wheat. In a similar study by Harmens et al. (2019) on wheat in Africa, grain yield loss due to O₃ exposure was greater in well-watered plants than in crops that received reduced irrigation suggesting controlled irrigation as a management tool to reduce O₃ impact. Whilst drought reduces yields at all stages of development, drought stress during anthesis and grain-filling cause the greatest yield reductions (Farooq et al., 2014). Additionally, anthesis and grain filling is when wheat is most sensitive to [O₃] and is the period of time when the [O₃] are highest during the Indian growing season (Gelang et al., 2000; Pleijel et al., 1998; Rathore et al., 2023). Several experimental studies have investigated the interaction between O₃ and drought stress in wheat. While some studies have observed no significant interactions between increased [O₃] and water stress (Broberg et al., 2023; Fangmeier et al., 1994), others have observed an interaction. Ghosh et al., (2020) observed an additive effect of O₃ and drought stress, with a greater reduction in grain yield when both stressors occurred simultaneously due to the reduction in nutrient uptake and assimilation. As a result of these contrasting findings, it is evident the trade-offs between O₃ exposure and water stress require further study. Irrigation has the potential to maximise O₃-stress by providing conditions likely to enhance stomatal conductance such as plentiful soil and leaf water, transpirational cooling and low leaf-to-air VPD. Irrigation is widespread across the IGP, particularly in the states of Punjab, Haryana and Uttar Pradesh; the area irrigated as a percentage of the total area of wheat was 99.1%, 99.9% and 99% respectively in 2018-19 (Ministry of Agriculture & Farmers Welfare, 2022), which means that current wheat crop management practices are likely to enhance sensitivity to O₃. Modifying irrigation practices has been suggested as a strategy to reduce O₃ damage, but caution is needed to avoid introducing water stress, which could also negatively affect yield (Harmens et al., 2019; Teixeira et al., 2011). Irrigation has additional benefits and has often been implemented to offset heat-related yield losses which occur when temperatures exceed 35°C (Zaveri and Lobell, 2019). However, studies suggest that sustainable use of India's future groundwater availability with current irrigation practices would mitigate less than 10% of the climate change impact on crop yield (Fishman, 2018). Additionally, water for irrigation purposes is limited; for example, Zaveri et al. (2016) found Uttar Pradesh will lack scope for further increasing irrigation as groundwater depletion escalates due to climate change and increased unsustainable water demand. With irrigation accounting for up to 90% of India's total water demand, water efficiency in agriculture is a priority in the IGP to achieve better environmental and economic performance (Fischer et al., 2007; Wada et al., 2013). Here, we explore the interplay between O₃- and water-stressed induced yield losses which will help inform whether water efficiencies could also provide some benefits in terms of the decreased sensitivity of staple crops to O₃.

98 There have been an increasing number of studies exploring the effect of O₃ on wheat yields using a cumulative stomatal O₃
99 flux metric (POD_Y; phytotoxic O₃ dose over a flux threshold Y) which accounts for the stomatal response to environmental
100 conditions and plant growth stages that alter O₃ uptake. By comparison, concentration-based exposure metrics such as AOT40
101 only account for atmospheric [O₃] which may be decoupled from O₃ uptake under environmental conditions that limit stomatal
102 conductance; they also omit O₃ below 40 ppb which are known to be capable of causing damage (CLRTAP, 2017; Emberson
103 et al., 2018). Mills et al. (2018a) estimated an O₃-induced yield loss that incorporated the effects of irrigation to be in the range
104 of 15–20% for wheat growing in Uttar Pradesh between 2010–2012 using POD₃IAM (POD above 3nmol m⁻²s⁻¹, parameterised
105 for integrated assessment modelling) (CLRTAP, 2017). This parameterisation was based on European wheat cultivars and a
106 broad-scale assessment of India's wheat growing season with the POD₃IAM metric being applied according to the formulations
107 of the Deposition of Ozone for Stomatal Exchange (DO₃SE) model (Büker et al., 2012; CLRTAP, 2017; Emberson et al.,
108 2000a, 2018). An alternative metric used in estimations of stomatal O₃ flux effects on crops is POD₆SPEC, which is the
109 species-specific phytotoxic O₃ dose above 6 nmol m⁻² s⁻¹. This metric is better suited for local-regional risk assessments
110 (CLRTAP, 2017).
111 Application of the stomatal O₃ flux method allows exploration of the relative effects of both O₃ and water stress on yield since
112 the DO₃SE model also estimates water vapour fluxes from which potential and actual evapotranspiration can be calculated
113 (Büker et al., 2012). In this study, we parameterise the DO₃SE 3.1.0 version model for two late-sown Indian wheat cultivars
114 for the estimation of POD₆SPEC metric. We apply the Weather Research and Forecasting model with Chemistry (WRF-Chem)
115 (Grell et al., 2005) to obtain [O₃] and climate variable data for Varanasi, Uttar Pradesh. We compare O₃ effect yield losses
116 (using the wheat grain yield flux-effect relationship (CLRTAP, 2017) with yield losses due to water stress based on yield
117 responses to the ratio of actual vs potential evapotranspiration (cf. FAO (2012)). This modelling set-up allows us to explore
118 the relative magnitude of yield losses from O₃ and water stress; how these are likely to change in the future and the relative
119 sensitivities of older vs more recently released Indian cultivars to damage from O₃ pollution.

120 2 Methods

121 For this study, Varanasi was selected as the study area due to (i) its location in the important wheat-growing IGP and, (ii) the
122 availability of observed crop and O₃ data.

123 2.1 Experimental data

124 Experimental data from 2016–2018 were obtained for two late sown Indian spring wheat (*Triticum aestivum* L.) cultivars
125 grown at the Botanical Garden, Banaras Hindu University (BHU), Varanasi (25°16' N, 82°59' E; 81.0m above sea level).
126 HUW-234 (released in 1986 by BHU, Varanasi) and HD-3118 (released in 2014 by IARI, New Delhi) were selected based on
127 their heat tolerance and extensive cultivation in the North East Plain Zone of India (Joshi et al., 2007; Yadav et al., 2019). The
128 recently released cultivar, HD-3118 is more high-yielding (6.64 tons ha⁻¹) compared to HUW-234 (4.5–5 tons ha⁻¹), most

Formatted: Subscript

Formatted: Superscript

Formatted: Superscript

likely due to its enhanced capacity for gas exchange. This enhanced capacity for gas exchange is the likely reason for the HD-3118 cultivar having a greater sensitivity to O₃ than the HUW-234 cultivar (Yadav et al., 2020).

2.2 Modelled data

Hourly meteorological [and O₃](#) data for the Varanasi grid box (45 km x 45 km horizontal resolution) were obtained by running WRF-Chem v.3.8.1 for years 1996-2005 ([considered the 'recent past current' climate](#)) and 2046-2055 using both RCP4.5 and RCP8.5 climate scenarios. The 45 km resolution model domain is the same as in Daloz et al. (2021), and the meteorological initial and boundary conditions come from global climate model simulations with the Community Earth System Model (CESM) v.1.0.4 (Gent et al., 2011), documented in Hodnebrog et al. (2019). The WRF-Chem simulations are set up with the RADM2 gas-phase chemistry scheme (Stockwell et al., 1990) [and O₃ precursor emissions are from Lamarque et al. \(2010\) for the historical period and from Lamarque et al. \(2011\) for the future RCPs](#). Global mean CO₂ mixing ratios (ppm) for 1996-2005 were obtained from NASA (using Tans and Conway (no date) for 1983-2003 and Conway (no date) for 2004-2007). For future scenarios, RCP4.5 and RCP8.5 [CO₂] for 2046-2055 were acquired (Meinshausen et al., 2011). [WRF-Chem with the RADM2 chemical mechanism has been found to reproduce diurnal average O₃ over India in February-May relatively well, while noontime O₃ concentrations show considerable differences between simulations with various emission inventories \(Sharma et al., 2017\).](#)

The RCP climate scenarios are selected to provide a range of climate and pollution futures for India from which a consequent range in yield responses can be estimated. RCPs are possible greenhouse gas (GHG) emission pathways designed to aid research into climate change impacts (Riahi et al., 2011). RCP8.5 is a very high baseline, representing the highest GHG emission pathway in a 'business as usual' scenario resulting in a radiative forcing of 8.5 Wm⁻² at the close of the 21st century; equivalent to 1370 ppm [CO₂] (He and Zhou, 2015; Riahi et al., 2011). RCP4.5 is a medium stabilisation scenario where global climate policy values the role of natural carbon sequestration and land use, resulting in a radiative forcing target of 4.5 Wm⁻² (650ppm [CO₂] equivalent) for 2100 (Riahi et al., 2011; van Vuuren et al., 2011).

These data provided input to the DO₃SE model which was used to simulate stomatal O₃ flux values and water stress characteristics for the two cultivars for each year. The modelled climate, O₃ and CO₂ data for the [recent past current-climate](#) and both RCP scenarios are summarised in Table 1. The modelled temperature data are on average 1.3°C warmer in the RCP4.5 scenario and 1.9°C warmer in the RCP8.5 scenario than the [recent past current-modelled climate](#).

Table 1: Modelled climate, [O₃] and [CO₂] data for the Varanasi grid box, used for the [recent past current-climate](#) and both future RCP scenarios (expressed as the range of 24-hour mean values, value in brackets indicates mean). The length of growing season is shown in days over two years and can be visualised in Fig. 2.

Parameter	Recent past Current climate	RCP4.5 (2046-2055)	RCP8.5 (2046-2055)
-----------	---	-----------------------	-----------------------

(1996-2005)			
Temperature (°C _e)	17.4-20.6 (18.9)	19.1-21.3 (20.2)	19.6-21.8 (20.8)
VPD (hPa)	8.3-14.4 (11.0)	12.5-17.5 (14.5)	11.1-18.1 (15.1)
Precipitation (total over growing season; mm)	72.4-393.4 (235.5)	35.1-184.4 (101.7)	0.93-234.0 (92.5)
[O ₃] (24 hour mean; ppb)	47.1-50.6 (48.6)	57.9-62.2 (60.5)	54.6-63.0 (59.7)
[CO ₂] (ppm)	362.6-379.5 (370.7)	476.3-498.5 (487.6)	518.6-570.5 (543.9)
Growing season (Days over 2 years)	339-468	339-466	339-473

159 **2.3 Model formulation - O₃ induced yield loss estimates**

160 The DO₃SE 3.1.0 version model (<https://www.sei.org/projects-and-tools/tools/do3se-deposition-ozone-stomatal-exchange/>)
 161 was used to estimate stomatal O₃ flux and subsequent O₃-induced yield loss for wheat. DO₃SE is a dry deposition model which
 162 takes into account the influence of climatic, soil and plant factors on stomatal conductance to estimate stomatal O₃ flux and
 163 determine the accumulated stomatal O₃ uptake during a specified growth period; POD_y (CLRTAP, 2017). The stomatal
 164 conductance (g_{sto}) multiplicative algorithm Eq. (1) used in DO₃SE estimates hourly g_{sto} to O₃ by modifying a species-specific
 165 maximum g_{sto} (g_{max}) according to environmental variables and is described in Emberson et al. (2000a, b).

166
$$g_{sto} = g_{max} \times [\min(f_{phen}, f_{O_3})] \times f_{light} \times \max\{f_{min}, (f_{temp} \times f_{VPD} \times f_{sw})\} \quad [1]$$

167 where g_{sto} and g_{max} are expressed as mmol O₃ m⁻² PLA s⁻¹. The factors f_{phen} , f_{O_3} , f_{light} , f_{temp} , f_{VPD} , f_{sw} and f_{min} represent
 168 the influence of phenology, [O₃], light, air temperature, VPD, soil water potential and minimum g_{sto} and are expressed in
 169 relative terms as a proportion of g_{max} (so have a value between 0-1). Functions describing these factors for environmental
 170 conditions are described in CLRTAP (2017) based on European wheat varieties; for f_{sw} (and to simulate g_{sto} for rainfed wheat)
 171 we assume a linear relationship between a relative g_{sto} of 1 and f_{min} at soil water potentials (SW) of -0.3 and -1.1 MPa (Ali
 172 et al., 1999; Morgan, 1984). To simulate the g_{sto} of irrigated wheat we simply assume that f_{sw} is always equal to 1.

173 Stomatal O₃ flux (F_{st} ; nmol m⁻² PLA s⁻¹) was calculated using Eq. (2).

174
$$F_{st} = c(zi) \times g_{sto} \times \frac{rc}{(rb+rc)} \quad [2]$$

175 where $c(zi)$ is [O₃] at the top of the canopy height i (m), rc and rb represent leaf surface and quasi-laminar leaf boundary
 176 layer resistances respectively, based on leaf dimension and wind speed (CLRTAP, 2017).

The species-specific POD_Y (POD_YSPEC) is estimated for the wheat accumulation period according to Eq. (3).

$$POD_YSPEC = \sum \left[(F_{st} - Y) \times \left(\frac{3600}{10^6} \right) \right] \quad [3]$$

where Y ($\text{nmol O}_3 \text{ m}^{-2} \text{ PLA s}^{-1}$) is subtracted from F_{st} (in $\text{nmol m}^{-2} \text{ PLA s}^{-1}$) when $F_{st} > Y$, during daylight hours; this Y value represents the assumed detoxification capacity of wheat to O_3 flux. The value is then converted to hourly fluxes by multiplying by 3600 and to mmol by dividing by 10^6 to give POD_YSPEC in $\text{mmol O}_3 \text{ m}^{-2} \text{ PLA}$ (CLRTAP, 2017). A Y value of $6 \text{ nmol m}^{-2} \text{ PLA s}^{-1}$ was used based on values for European wheat (CLRTAP, 2017). The resulting POD_6SPEC values were used to estimate the percentage grain yield (relative to 100% grain yield under pre-industrial O_3 conditions) based on the dose-response relationship in Eq. (4).

$$\% \text{Grain Yield} = 100.3 - (3.85 \times POD_6SPEC) \quad [4]$$

The relationship in Eq. (4) is taken from CLRTAP (2017)/Grunhage et al. (2012) where relative grain yields from 5 wheat cultivars in 4 European countries were regressed against the POD_6SPEC value.

2.4 Model formulation - water stress induced yield losses

The DO_3SE 3.1.0 model was also used to model the effect of water stress on yield through the provision of estimates of potential (ET_m) and actual (ET_a) evapotranspiration following the DO_3SE model algorithms used to estimate soil-plant-atmosphere cycling of water described in B  ker et al. (2012). These DO_3SE algorithms essentially estimate the total loss of soil water through ET_a (and the equivalent ET_m) using the method of Shuttleworth and Wallace (1985) modified to incorporate the atmospheric, boundary layer and stomatal resistances to water vapour flux as calculated within DO_3SE . Resistances are scaled from leaf to canopy using LAI and upscaling methods described in B  ker et al. (2012). LAI is modelled to vary over the course of the wheat growing season between a value of 0 and $3.5 \text{ m}^2/\text{m}^2$ (consistent with average maximum LAI values frequently found across the IGP region as observed from satellite data (Nigam et al., 2017)). The DO_3SE soil moisture module was developed based on the Penman-Monteith model of actual evapotranspiration (Et_a), which is described in Eq. (5) (B  ker et al., 2012; Monteith, 1965; Shuttleworth and Wallace, 1985):

$$Et_a = \frac{\Delta (\Phi n - G) + \rho_a c_p \left(\frac{D}{R_{bH_2O}} \right)}{\lambda \left\{ \Delta + \gamma \left(1 + \frac{R_{stoH_2O}}{R_{bH_2O}} \right) \right\}} \quad [5]$$

where Δ is the slope of the relationship between the saturation vapour pressure and temperature, Φn is the net radiation at the top of the canopy, G is the soil surface heat flux, ρ_a is the air density, c_p is the specific heat of air, D is the vapour pressure deficit of air, R_{bH_2O} is the canopy boundary layer resistance to water vapour exchange, R_{stoH_2O} is the stomatal canopy resistance to the transfer of water vapour (the inverse of stomatal conductance to water vapour), γ is the psychrometric constant, and λ is the latent heat of vaporisation.

The effect of ET_a (and hence water-stress) on wheat yield was estimated according to the relationship between relative yield and the corresponding relative evapotranspiration (Et) described in Doorenbos and Kassam (1979) for spring wheat. When a

Formatted: Subscript

crop is not water-stressed, ET_a is equal to ET_m however in drought conditions, $ET_a < ET_m$ (Yao, 1974). The ET_a and ET_m values produced by DO₃SE were used in Eq. (6).

$$1 - \frac{Y_a}{Y_m} = K_y \left(1 - \frac{ET_a}{ET_m} \right) \quad [6]$$

where Y_a is the actual relative grain yield and Y_m is the potential relative grain yield. K_y is the crop-specific yield response factor assumed to be 1.15 for the whole growing season, in accordance with the value for spring wheat from the FAO (Steduto et al., 2012).

2.5 Model parameterisation

The DO₃SE model was parameterised for the HD-3118 and HUW-234 cultivars by (Yadav et al. (2021) using data from a series of O₃ exposure experiments at the Banaras Hindu University, Varanasi, Uttar Pradesh. For this study, we use the same parameterisation except for the f_{phen} term (which we allow to vary as a function of effective temperature sum (ETS) during the growing season) and the inclusion of the f_{O_3} term (which accounts for O₃ inducing early onset senescence). The parameterisations used for both cultivars are given in Table 2.

Table 2: Parameterisation of the DO₃SE model for POD₆SPEC for wheat flag leaves for Indian bread wheat (*Triticum aestivum* L.) cultivars. European bread wheat parameters reported by CLRTAP (2017) have been included for comparative purposes. Parameters are highlighted where there are differences between Indian and European cultivars.

Bread wheat cultivar parameterisation - POD ₆ SPEC				
Parameter	Units	Indo-Gangetic Plains		Atlantic, Boreal, Continental bread wheat (CLRTAP, 2017)
		HUW-234	HD-3118	
g_{max}	mmol O ₃ m ⁻² PLA s ⁻¹	500	521	500
f_{min}	fraction	0.13	0.13	0.01
light_a	-	0.011	0.011	0.011
T _{min}	°C	12	12	12
T _{opt}	°C	26	26	26
T _{max}	°C	40	40	40

Formatted Table

VPD _{max}	kPa	3.2	3.2	1.2
VDP _{min}	kPa	4.6	4.6	3.2
ΣVPD _{crit}	kPa	16	16	8
PAW _t [*]	%	50	50	50
f _{O3}	POD ₀ mmol O ₃ m ⁻² PLA s ⁻¹	14	14	14
Leaf dimension	cm	2	2	2
Canopy height	m	1	1	1
f _{phen_a}	fraction	0.3	0.3	0.3
f _{phen_e}	fraction	0.7	0.7	0.7
f _{phen_1_ETS}	°C day	-616.6	-553	-200
f _{phen_2_ETS}	°C day	0	0	0
f _{phen_3_ETS}	°C day	621.5	553	100
f _{phen_4_ETS}	°C day	182.75	238	525
f _{phen_5_ETS}	°C day	959	1000	700

223 ^{*}PAW_t is the threshold for plant available water (PAW) in mm above which stomatal conductance is at a maximum

224
 225 The ETS model (see Eq. 7) was calibrated using experimental data for HUW-234 and HD-3118 that provided the timing (as
 226 day of year) of key crop development stages (sowing, emergence, flag leaf emergence, fully expanded flag leaf, start of seed
 227 setting, start of senescence and harvest) for both cultivars for 3 years (2016 to 2018 inclusive). Corresponding 3-hourly
 228 temperature data were used to estimate daily mean temperature from which ETS values could be determined according to
 229 Eq. (7).

230 $ETS = \sum (T_i - T_b)$ [7]

Where T_i is the mean daily temperature and T_b is the base temperature assumed 0°C for wheat. This is equivalent to the method of thermal time accumulation recommended by CLRTAP (2017) and assumes that there is no upper threshold temperature for phenology and that thermal time increases linearly across the entire temperature range. The ETS components of the f_{phen} function from flag leaf emergence were estimated by assuming that f_{phen1_ETS} and f_{phen3_ETS} together were equivalent to thermal time equally divided between the emerging flag leaf and seed setting. This precaution ensured f_{phen} was not allowed to decrease too early; that f_{phen5_ETS} less f_{phen4_ETS} was equivalent to the thermal time at seed setting less the thermal time at flag leaf emergence and that f_{phen1_ETS} and f_{phen5_ETS} together were equivalent to the thermal time at harvest less the thermal time at flag leaf emergence; these basic assumptions allowed the derivation of f_{phen_ETS} parameters 1-5 given in Table 2. Supplement Figure S1 gives an indication of the year-to-year variability in the timing of these key growth stages used to parameterise the f_{phen} function. This f_{phen} function is subsequently used to represent the phenological influence on g_{max} and to define the seasonal accumulation period for POD_ySPEC (see also CLRTAP (2017)). Parameterisation of the f_{phen_ETS} model shows little difference in phenology between these cultivars, although HUW-234 had a greater range in dates of flag leaf emergence and fully expanded flag leaf. Seed setting and the start of senescence occurred ~3 days earlier in HD-3118 than HUW-234. The Indian cultivar f_{phen_ETS} values differ from the European Continental bread wheat values (also shown in Table 2). In part, this is related to the precautionary approach taken in defining the length of the period during which f_{phen} will equal 1 to ensure we capture the period when O₃ may be taken up by the stomata in the absence of growth stage data more specific to the f_{phen_ETS} stages. The resulting f_{phen_ETS} parameterization suggests that Indian cultivars take more thermal time to reach mid-anthesis and less thermal time between the start of senescence and harvest than would bread wheat from the European region.

2.6 Model runs

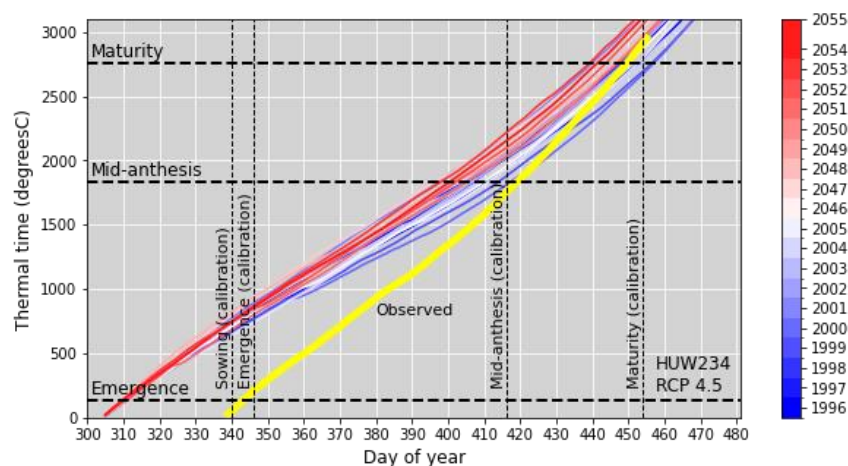
DO₃SE 3.1.0 model runs were made for each cultivar described in Table 2 using the WRF-Chem modelled O₃ and met data for 1996-2005 which was assumed to represent the **recent past current-climate**. The DO₃SE model runs were repeated for future scenarios using the WRF-Chem modelled O₃ and meteorological data for 2046-2055 based on the two scenarios; RCP4.5 and RCP8.5 to explore the influence of changes in climate and O₃ precursor emissions on O₃ uptake. We assume a sowing **datedata** of early November since October to December represent the main sowing months of wheat across the most productive wheat growing states in the IGP (Lobell et al., 2013).

3 Results and discussion

3.1 Phenology and stomatal O₃ uptake

Accurate modelling of the growing season and the f_{phen} period in relation to the prevailing O₃ climate is crucial for realistic estimates of O₃ damage to wheat. The ETS model for late-sown cultivars is variable in its ability to simulate key growth

261 stages between years and cultivars. For each growth stage, the minimum and maximum °Cday values between years are 63 to
 262 426°Cday for HUW-234 and 63 to 317°Cday for HD-3118 respectively. Given that the mean daily temperature during the
 263 Indian wheat growing season is ~25°C this would suggest the ETS model may have a maximum error of 17 and 13 days for
 264 HUW-234 and HD-3118 respectively. These values are likely at the high end of the uncertainty range as temperatures
 265 increase during the growing season and the greatest uncertainty was found for the flag leaf emergence and fully expanded
 266 flag leaf growth stages. The inclusion of the ‘emerging flag leaf’ in the f_{phen} period helps to capture the full period when the
 267 flag leaf may be vulnerable to O₃ as a precaution given the uncertainty in the ETS model defining the timing of the period
 268 from full flag leaf expansion and senescence.

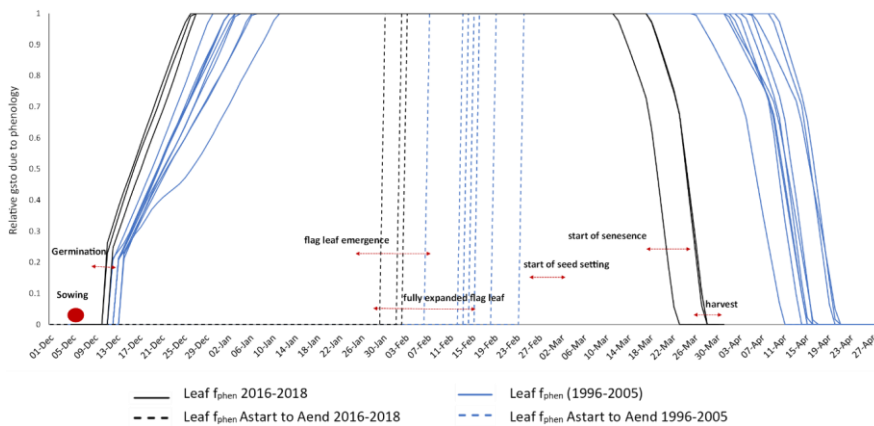


269
 270 **Fig. 1: The evolution of ETS and associated growth stages for the observed (2016-18) climate (to which the ETS model is calibrated**
 271 **with a sowing date of 5th Dec) and the WRF-Chem modelled recent past current (1986-2005) and future (2046-2055; RCP4.5 and**
 272 **8.0) climates (for which the model is applied with a sowing date of 5th Nov) for the HUW-234 cultivar.**

273 When the parameterisation was applied to the WRF-Chem modelled 1996-2005 climate temperature data, with a sowing date
 274 of 5th November, maturity is simulated to occur around the end of March (consistent with our observed maturity date of the
 275 late sown variety under the relatively high temperatures for years 2016-2018 used for parameterisation) – see Fig. 1. Thus
 276 our f_{phen} parameterisation, when using standard, early November, sowing dates gives realistic maturity dates for IGP grown
 277 wheat when used with recent past current-year WRF-Chem modelled data (Fig. 2). Since the WRF-Chem data are consistent
 278 between climate periods (i.e., 1996-2005 and 2046-2055) they can be deemed to provide a means of comparing the relative
 279 effect of changes in temperature on the growing season, O₃ uptake and the evolution of soil moisture deficit.

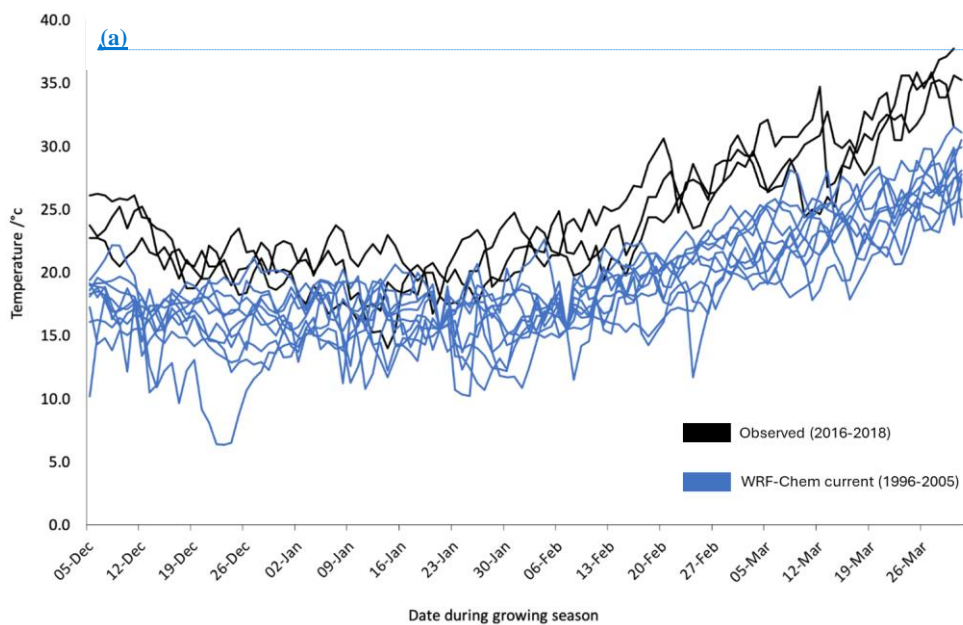
280 The empirical data used for model parameterisation collected in years 2016-18, consistently produced higher temperatures
 281 than the WRF-Chem model-based meteorological data, which was collected from 1996-2005 (Fig. 3a). This could be in part

282 due to climate change; average air temperatures in India for 2016, 2017 and 2018 were in the top ten on record since 1901
 283 (ESSO, 2019). However, on average, 2016-18 was only +0.72°C, +0.55°C and +0.41°C warmer than the 1981-2010 annual
 284 air temperature average respectively (Earth System Science Organisation et al., 2019), therefore it is likely that uncertainties
 285 in the modelled values caused the greater part of these discrepancies in temperatures. Since the WRF-Chem model at this
 286 resolution may not consider some urban heat island effects, a finer model resolution may have led to better agreement with
 287 observations for this urban site. Despite this, the nature of the ETS model is that it can provide comparative estimates of the
 288 influence of temperature profiles on the timing and length of the growing season. [Fig 3b shows a similar comparison](#)
 289 [between WRFChem modelled O₃ concentrations \(provided as 5 year mean hourly values with absolute minimum and](#)
 290 [maximum bounds also shown\) and the ambient air \(AA\) O₃ concentration data for the 2016-2017 wheat growing season of](#)
 291 [the O₃ experiment. This shows that the WRFChem modelled past climate \(1996-2005\) data is within range, but at the lower](#)
 292 [end, of the 2016-17 O₃ experimental data as would be expected given the increase in O₃ precursor emissions over the past](#)
 293 [few decades.](#)
 294



296 Fig. 2: The ETS model parameterised for HUW-234 based on observed [recent past current](#)-temperatures (2016-2018; black). The
 297 ETS model for the modelled [recent past current](#)-temperatures (years 1996-2005) are in blue. The range of observed dates of
 298 sowing, germination, flag leaf emergence, fully expanded flag leaf, start of seed setting, start of senescence and harvest from the
 299 experimental data (Agrawal, pers. comm.) are marked with arrows. Astart to Aend represent the start of anthesis to the end of
 300 anthesis.

305
306
307
308
309
310
311



Formatted: Font: 12 pt, Bold

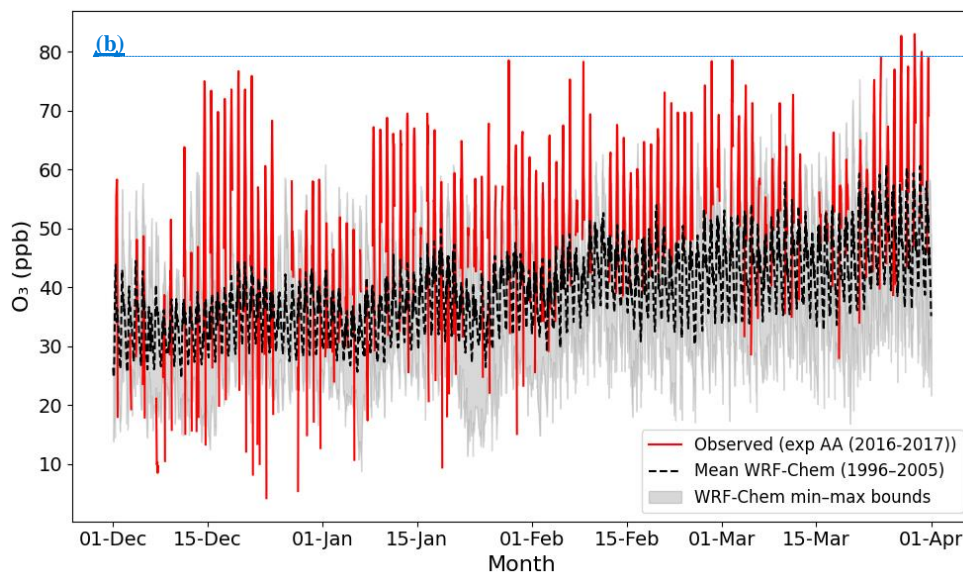


Fig. 3: Seasonal profiles of (a) T_{surface} temperatures changes over the growing season for observed calibration data (2016-18) and WRF-Chem modelled data for the recent past current climate (1996-2005), and (b) O₃ concentration over the growing season for observed data (exp AA (experiment ambient air) for Dec 2016 to Mar 2017 and 10 year (1996 - 2005) annual mean WRF Chem modelled O₃ concentration data with associated absolute minimum and maximum O₃ concentrations bounds also shown.

The DO₃SE wheat stomatal O₃ flux model has been evaluated against wheat g_{sto} data (the primary determinant of stomatal ozone flux) collected under experimental conditions in Ostad, Sweden (Pleijel et al. 2007) and found to perform well (with an R² value of 0.83 for a regression of observed against modelled g_{sto}). The DO₃SE model has also been extensively evaluated for a number of crops at locations around the world (as reported in Tuovinen et al. (2004) for wheat growing near Cumono novo in Italy and Emmerichs et al. (2025) for wheat growing near Grignon in France). These evaluations rely on total O₃ flux and deposition measurements (since they use O₃ flux tower data) or water vapour flux measurements and thereby test whole canopy fluxes rather than the representative upper leaf stomatal flux required for PODy calculations. However, the combination of these evaluation methods focussing on both leaf level g_{sto} and canopy level O₃ flux together provide confidence in the predictive abilities of the DO₃SE model.

3.2 Effect of O₃ stress on the yield benefits of irrigation

Water-stress induced yield loss under rainfed conditions modelled under the climate scenario for 1996-2005 was found to exceed O₃-related yield loss (O₃-RYL) under irrigated conditions for the majority of the 10 years investigated. Under this climate, rainfed conditions produced a mean water-stress related yield loss (WS-RYL) of 13.3% for HUW-234, with a

Formatted: Font: 12 pt, Bold

Formatted: Font: 12 pt, Bold

Formatted: Subscript

Formatted: Line spacing: 1.5 lines

Formatted: Subscript

Formatted: Subscript

Formatted: Subscript

Formatted: Subscript

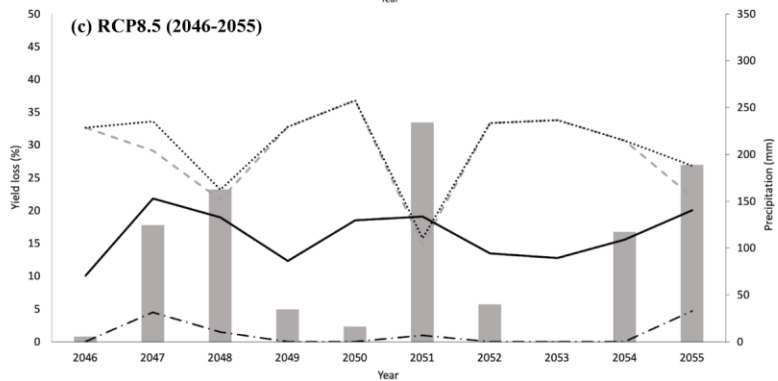
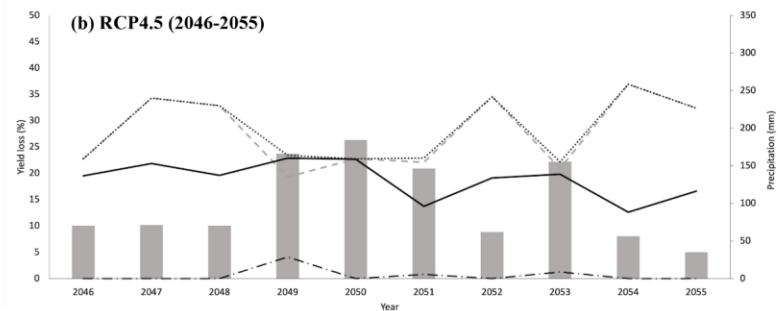
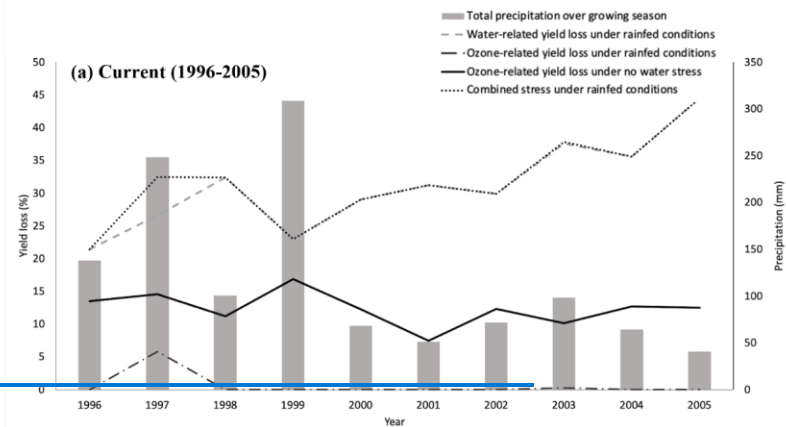
Formatted: Subscript

Formatted: Font: 10 pt, Not Bold, Font color: Auto

332 range of 2.8-31.3% (Fig. 4a). Under rainfed conditions, mean O_3 -RYL was projected to be negligible (0.6%), significantly
333 lower than the mean O_3 -RYL when no water-stress is assumed under irrigation (10.7% with a range of 4.8-15.4%). This
334 demonstrates the importance of irrigation for wheat production in India and highlights the substantial influence on the yield of
335 O_3 for irrigated wheat.

336 O_3 -RYL under irrigated conditions exceeded WS-RYL in 80% of the 10 years investigated in the RCP4.5 scenario (Fig. 4b).
337 This highlights how O_3 stress negates some of the increased productivity that arises from reducing water stress through
338 irrigation. In the RCP8.5 scenario, WS-RYL under rainfed conditions exceeded O_3 -RYL under irrigated conditions in all but
339 one year (2051), when precipitation totaled 234.0mm for the growing season (Fig. 4c). In this scenario, precipitation during
340 the growing season ranges from 0.9-234.0mm, with a mean of 94 ± 82.97 mm, and as a result the WS-RYL fluctuates within the
341 10 years.

342 Whilst irrigation has played an important role in increasing yields for India's wheat, these results show that O_3 is likely to
343 negate some of the yield benefits of irrigation. Based on the results of simulations of future climates, irrigation will have less
344 of an effect on yield increases as $[O_3]$ levels rise.



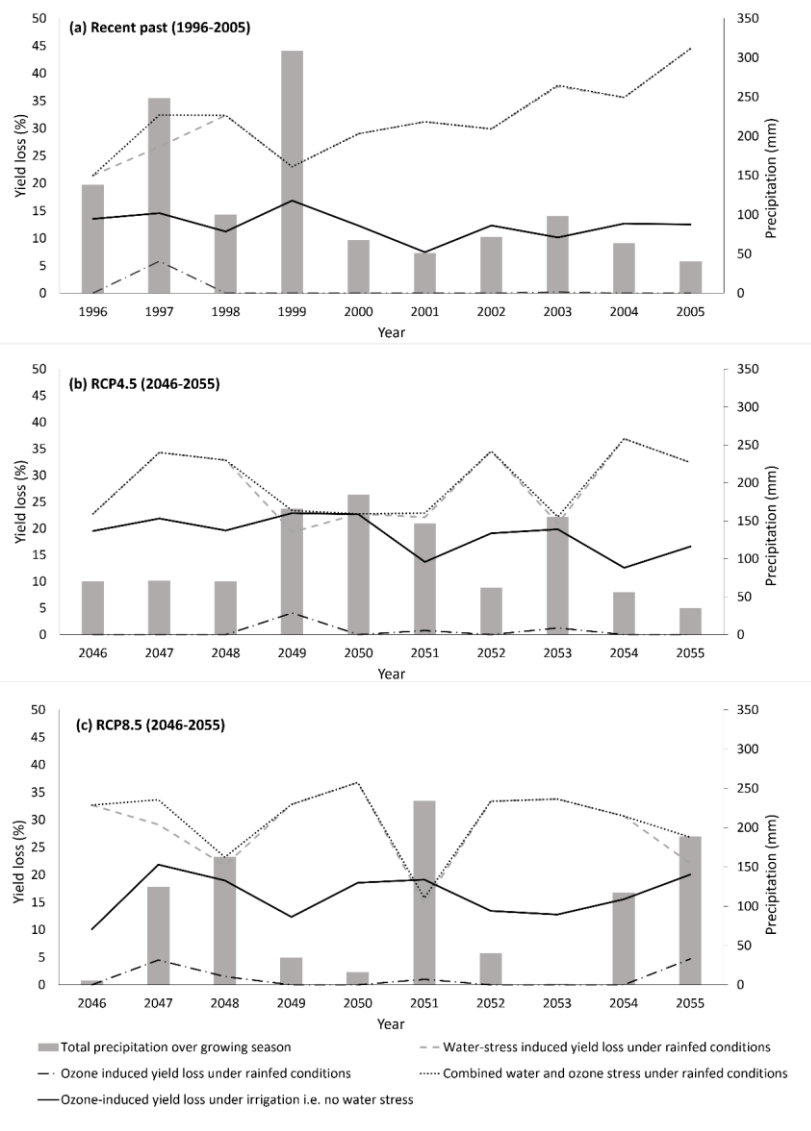


Fig. 4: The water-stress and ozone-related relative yield loss modelled for HUW-234 under rainfed conditions (water stress) and with no water stress (f_{sw} set to 1 in DO₃SE) for (a) the ~~recent past~~ ~~current~~-climate 1996-2005; (b) RCP4.5 scenario 2046-2055; (c) RCP8.5 scenario 2046-2055.

The mean total precipitation for the growing season under the 1996-2005 climate scenario was higher than the median values in the RCP4.5 and RCP8.5 scenarios for 2046-2055, meaning Uttar Pradesh's crops will receive less rainfall in the future. In addition, the RCP8.5 scenario had a larger interquartile range (IQR) of 131.0mm than the 1996-2005 climate (54.8mm) and the smallest lower quartile (22.3mm), demonstrating less and more irregular precipitation in the future climate. Whilst RCP4.5 was less extreme; it had a larger IQR of 90.1mm. This irregularity and increased risk of low precipitation over the growing season demonstrates the continuing importance of irrigation for wheat productivity. In all modelled climate scenarios, water stress tends to be a much greater threat to crop yields than O₃ and therefore, some level of irrigation is crucial for sustained wheat productivity in India. However, these findings clearly show that O₃ is a limiting factor to yield under irrigated conditions meaning that the full potential benefit of irrigation is not being realised and hence will lead to inefficiencies in the use of irrigation water. Further research should be carried out to find the 'sweet spot' for irrigation, that will minimise O₃ stress without inducing water stress, to practice more responsible water management.

Future studies should investigate how short, sharp high O₃ periods could be mitigated with temporary reductions in irrigation, if the efficacy of such approaches can be demonstrated they could be practically applied in the future with the advent of new technologies such as accurate pollution forecasting via machine learning models (Jumin et al., 2020; Wang et al., 2020). A holistic approach that considers the trade-offs between other abiotic stressors such as heat stress is needed, as irrigation plays a significant role in mitigating such stress (Zaveri and Lobell, 2019) and higher temperatures are a precursor of higher O₃ levels with the chance that O₃ effects are erroneously attributed to heat stress (Tai et al., 2014).

3.3 Effect of climate change on O₃ sensitivity

Higher O₃-induced yield losses were modelled under future scenarios (Fig. 5). For HUW234, a statistically significant increase in yield loss of 7.9±5.56% and 3.1±5.08% was modelled for RCP4.5 and RCP8.5 respectively, compared to the ~~recent past~~ ~~current~~-climate. Similarly, for RCP4.5 and RCP8.5, an increase of 8.0±5.71% and 3.0±4.87% yield loss was predicted for HD-3118, respectively. This suggests that the increase in O₃ impact due to future emissions/climate is larger than the year-to-year variability in O₃ impact for the RCP4.5 (but not RCP8.5 where [O₃] were lower, see below) scenario. The ~~recent past~~ ~~current~~ climate represents the lowest mean O₃, suggesting O₃, rather than other environmental conditions that might influence sensitivity to O₃, (*i.e. via alterations to stomatal O₃ uptake*)-is the most important factor in determining O₃-induced yield loss. These findings imply that the changing climate (*i.e.*, higher frequency of temperatures that exceed the T_{opt} with consequent reductions in stomatal conductance and hence O₃ flux) will be insufficient at ameliorating the increase in O₃-induced yield loss. This contrasts with several studies that have shown the potential of elevated temperatures to lead to reductions in O₃ flux via reduced stomatal conductance, thus reducing O₃ damage (Emberson et al., 2018; Feng et al., 2008). This could be due to differences in the timing and duration of periods of more extreme temperatures that exist between studies; a possibility that

380 would benefit from further study. It is important to clarify that in this study we explore future changes in ozone concentration
 381 due to changes in climate due to changes in O_3 precursor emissions. O_3 studies often explore the effect of a ‘climate
 382 change penalty’ which is the impact of a future climate on O_3 levels if emissions are held constant (Wu et al., 2008; Zanis et
 383 al., 2022). Although this is not specifically investigated in this study it is worth noting that India is one of the global regions
 384 with the strongest effect of a ‘climate change penalty’ (Zanis et al 2022). Given the interplay between climate and O_3 in
 385 determining the extent of stomatal O_3 uptake, and hence crop sensitivity to O_3 , it is worth noting that even without changes in
 386 emissions, O_3 -induced crop damage would still be likely to change to some extent under future conditions.

Formatted: Subscript

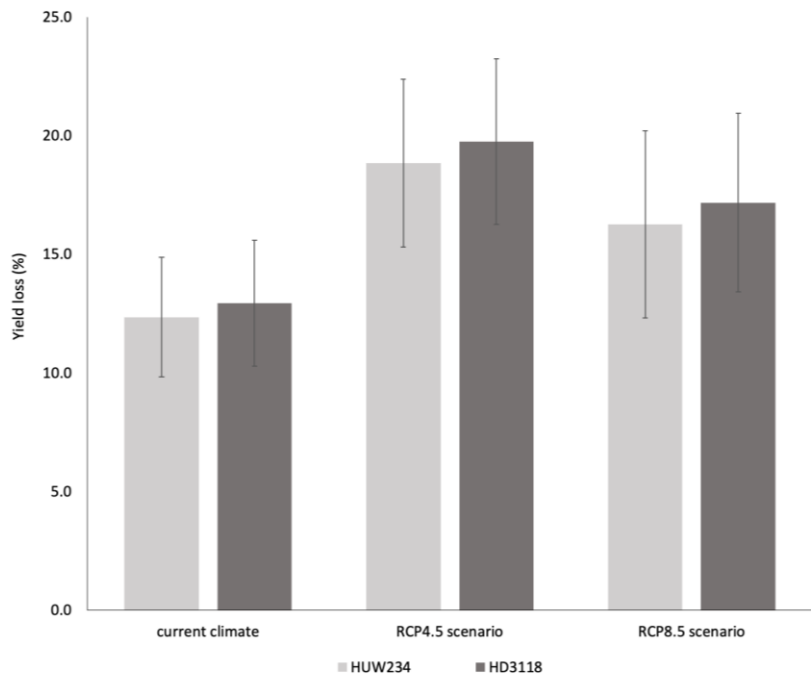
Formatted: Subscript

Formatted: Subscript

Formatted: Subscript

Formatted: Subscript

Formatted: Subscript



387
 388 Fig. 5: Mean O_3 -induced relative yield losses (O_3 -RYL) \pm SD modelled for the ~~recent past~~ ~~current~~ climate (1996-2005), and two future
 389 climate scenarios for 2046-2055; RCP4.5 and RCP8.5 for two Indian spring wheat cultivars; HUW-234 and HD-3118.

390 The results from this study are within the range published by Mills et al. (2018b) for O_3 -induced yield losses for wheat in Uttar
 391 Pradesh, which were modelled for 2010-2012 using POD_3 IAM with European wheat parameterisation and a broadscale
 392 assessment of India’s wheat growing season. The Mills et al. (2018b) study used the most recent methodology from CLRTAP

(2017) to calculate O₃-induced yield loss for wheat, as a reference POD₃IAM value representing O₃ uptake at pre-industrial conditions was subtracted before crop loss was calculated. Whilst this study also uses a stomatal flux-based metric, POD₃IAM is vegetation-type specific suited for large-scale modelling (CLRTAP, 2017). The POD₆SPEC was used in this current study since we were able to define a cultivar-specific growth period with some certainty thereby allowing greater confidence in the use of the more biologically relevant metric than POD₃IAM (CLRTAP, 2017). It is also worth noting that the timing of O₃ and water stress may be important in predicting how plants respond to these stresses since O₃ has been found to damage stomatal functioning causing plants lose the ability to respond to water stress (e.g. Wilkinson et al., 2010). Ideally, O₃ impact models would include mechanisms that simulate O₃-induced loss in stomatal functioning, however, to our knowledge such modelling mechanisms have not yet been developed or included and would likely require experimental data to identify thresholds at which stomatal functioning is impaired.

Mean relative O₃ induced yield losses for both cultivars modelled under RCP4.5 (18.7±3.83%) were significantly higher than the RCP8.5 (13.8±3.22%). This is likely due to a combination of slightly higher [O₃] in RCP4.5 (Table 1) and the WRF-Chem model projections of higher temperatures (limiting O₃ flux as temperatures have a tendency to exceed T_{opt}) under RCP8.5. Whilst the RCP4.5 scenario sees a global reduction in [O₃] due to pollution regulation, the South Asian region is an exception to this rule, where [O₃] continues to increase at a similar rate as occurred in previous decades (Tai and Martin, 2017). RCP8.5 projects a worldwide increase in [O₃] due to the lack of regulation of precursor emissions except in parts of the US, East and Southeast Asia (Tai and Martin, 2017). Therefore, mean [O₃] during the growing season is lowest in the recent past current climate at 48.6ppb but similar, at least in South Asia, in both the RCP4.5 and RCP8.5 scenarios (60.5ppb and 59.7ppb respectively; Table 1).

Relatively small differences in 2000-to-2050 increases in O₃ over South Asia between RCP4.5 and RCP8.5 have also been found before (Tai et al., 2014; their Supplementary Figure 1). Our WRF-Chem model results do show a slightly higher increase in O₃ precursors over India in RCP4.5 than RCP8.5 (not shown), likely explaining the slightly higher O₃ increase in the RCP4.5 scenario. However, several factors influence the modelled future O₃ concentration changes, such as the future change in meteorological variables, the non-linearities of O₃ chemistry, and natural interannual variability. For example, Sharma et al. (2023) found underestimation of relative humidity in meteorological data used in O₃ simulations which will have some influence on O₃ production estimates. Future studies should utilize emission scenarios that are more updated in terms of air pollution policies.

The O₃-induced yield loss will increase from current levels, regardless of whether global emissions follow a business-as-usual or medium stabilisation scenario. We predict that O₃-induced yield losses will continue to increase in South Asia with climate change, given the co-emission of radiative forcers and O₃ precursors and the two-way causality that exists between O₃ formation and climate change, i.e., hot, sunny conditions likely to be enhanced under climate change encourages O₃ formation, whilst O₃ itself is a radiative forcer (Fu and Tian, 2019). This means that O₃ and climate variable stress are likely to co-occur in the future which becomes especially problematic for crop productivity when environmental thresholds (e.g. due to temperature extremes) for plant productivity are exceeded. South Asia and the IGP are important agricultural regions where

Formatted: Subscript

Formatted: Subscript

Formatted: Subscript

Formatted: Subscript

Formatted: Subscript

Formatted: Subscript

Formatted: Subscript

Formatted: Subscript

Formatted: Subscript

Formatted: Subscript

Formatted: Subscript

O₃ thresholds are being exceeded now (Mills et al., 2018c), with the likelihood that the extent of such exceedance will only worsen in the future and with climate change (Cooper et al., 2014; Fowler et al., 2008; Fu and Tian, 2019; Rathore et al., 2023). It should be noted that there are uncertainties in the WRF-Chem model used in modelling meteorological and [O₃] data. There are important criticisms that the WRF-Chem model is limited in its ability in capturing true wind speeds, which influences temperature and O₃ mixing ratios (Rydsaa et al., 2016). Despite this, these findings serve as a useful insight into the future risk of O₃ on wheat yields relative to early 21st-century conditions. Ideally, future research should consider the use of model ensembles to more robustly capture ranges in future meteorological and [O₃] data.

3.4 Influence of cultivar physiology on O₃ sensitivity

The O₃-RYL modelled for HUW-234 were similar to HD-3118 in the ~~recent past current~~-climate and both the RCP4.5 and RCP8.5 scenarios (Fig. 5). This is due to the similarity in g_{max} values for HUW-234 and HD-3118 which were estimated, from empirical data at 500mmol O₃ m⁻² PLA s⁻¹ and 520.9 mmol O₃ m⁻² PLA s⁻¹ respectively. The mean yield losses for ~~recent past current~~-climate and RCP scenarios combined, modelled for HD-3118 (14.5±0.05%) were similar to HUW-234 (14.3±0.05%), a difference of 0.2%. Despite the similar mean yield losses observed for HD-3118 and HUW-234, these results align with concerns that modern wheat cultivars are more susceptible to O₃-damage as they are bred for maximum gas exchange or heat tolerance rather than O₃ tolerance (Emberson et al., 2018; Pleijel et al., 2006; Yadav et al., 2020). Typically, plant traits bred for heat tolerance and maximum gas exchange conflict with traits for O₃ tolerance and may increase irrigation requirements; i.e. higher stomatal conductance enhances transpiration rates, allowing for higher rates of photosynthesis (Pleijel et al., 2007; Yadav et al., 2020). Despite the potential for HD-3118 to produce higher yields due to a high stomatal conductance, HUW-234 performs better in terms of O₃ tolerance for Varanasi's ~~recent past current~~-conditions and projections for the future climate and [O₃]. This is also observed in the empirical data for Varanasi from 2016-18, which was used to parameterise the ETS model. The empirical data observed lower relative yield loss under elevated [O₃] compared to ambient [O₃] for HUW-234 than HD-3118 (21.2% and 23.2% respectively; see Table S1). Absolute yields failed to observe the higher yielding potential expected of HD-3118 even under ambient conditions; the mean absolute grain yield for HUW-234 under ambient [O₃] was 533.4g/m compared to 432.8g/m for HD-3118. Under elevated [O₃], the yield gap widens; HUW-234 has an absolute grain yield of 420.4g/m whilst HD-3118 has a yield of 332.3g/m. This suggests O₃ has a greater impact on yield in HD-3118 than HUW-234, possibly even under ambient concentrations.

Despite corroborating literature for the DO₃SE model results (Yadav et al., 2020), there is some limitation in the ability to accurately parameterise the model for specific cultivars. Here we have been able to parameterise key parameters that will influence stomatal O₃ flux (g_{max} and f_{phen}) for Indian varieties, however, the remaining parameters that determine the modification of g_{max} by environmental conditions rely on European parameterisations. Similarly, the DO₃SE model estimates O₃-induced crop yield losses based on a dose-response relationship configured using five European wheat cultivars (CLRTAP, 2017). Whilst the DO₃SE model is a valuable tool for risk assessment, the use of appropriately calibrated and evaluated crop models will provide mechanisms to fully explore the interplay between stresses such as O₃ and water stress on yield (Emberson

et al., 2018). The results of this paper make clear the need for such modelling to improve our understanding of how these different stresses act over the course of the growing season to determine changes in productivity. A new generation of crop models that are being developed to incorporate the O₃ effect, as well as other stresses (Emberson et al., 2018), will be able to explore trade-offs between stresses related to soil water, extreme temperatures, and soil fertility. Such advances in crop modelling will be crucial in assessing future wheat productivity under a range of abiotic stress conditions. In this Indian study, the mid-anthesis and grain filling period occurred in March (Fig.'s 1 and 2) which corresponds to peak O₃ in Uttar Pradesh (Jain et al., 2023; Mukherjee et al., 2019; Shukla et al., 2017). However, a study on timely-sown Chinese winter wheat cultivars found that elevated O₃ only had a significant effect during the mid-grain filling stage, suggesting that timing mid-grain filling with O₃ troughs could be a mitigation strategy, which may be achieved by earlier sowing (Feng et al., 2016). Late planting results in reduced productivity of the wheat crop, with earlier, timely sowing of wheat in the third week of November yielding the best productivity in Eastern Uttar Pradesh (Chandna et al., 2004). Past studies have reported that delays in sowing after mid-November leads to reduction in yield of wheat, often at a rate of 1-1.5% per day (McDonald et al., 2022; Ortiz-Monasterio R. et al., 1994). In addition, Kumar et al. (2014) claimed conversion from late to timely-sown would offset the impacts of climate change. A multi-tolerance approach like early sowing could mitigate heat and O₃ stress however, late sowing is often due to delays in harvesting rice in Rice-Wheat systems, a cropping sequence which provides income for tens of millions of farm families (Jain et al., 2017; Mishra et al., 2021). Further investigation of the inter-play between [O₃] profiles over the growing season and targeted crop phenology of different cultivar types should be conducted.

4 Conclusion

Whilst irrigation has played a pivotal role in increasing wheat production in India through maximising yields, O₃ is likely to negate some of the yield benefits of irrigation, which will reduce irrigation efficiency. Based on the POD₆SPEC values obtained *via* the DO₃SE model and associated flux-response relationships, O₃ concentrations prevalent in the IGP region of India are high enough to cause grain yield losses in Indian wheat. This paper demonstrates the complexity of avoiding O₃-stress and the importance of taking a multi-stress approach to mitigation. Since high levels of O₃ typically coincide with other abiotic stressors such as heat stress, the approach taken to maximise crop yield must consider multiple stressors and their interactions. Rather than altering irrigation patterns to mitigate O₃ stress and risk increasing the effect of other stressors such as water stress or heat stress, earlier sowing to avoid peak O₃ and temperatures in March may benefit irrigated wheat growing in India. Given that modern wheat cultivars are more O₃-sensitive, wheat growers should reconsider using modern cultivars bred for optimal gas exchange.

Competing interests

The contact author has declared that none of the authors has any competing interests

491 **Acknowledgements**

492 Funding from The Norwegian Research Council funded CICERO strategic project (grant no. 160015/F40) and the CiXPAG
493 project (grant no. 244551) provided support to Lisa Emberson, Øivind Hodnebrog and Madhoolika Agrawal.

494 **References**

- 495 Ainsworth, E. A., Rogers, A., and Leakey, A. D. B.: Targets for crop biotechnology in a future high-CO₂ and high-O₃ world,
496 *Plant Physiol.*, 147, 13–19, <https://doi.org/10.1104/pp.108.117101>, 2008.
- 497 Ali, M., Jensen, C. R., Mogensen, V. O., Andersen, M. N., and Henson, I. E.: Root signalling and osmotic adjustment during
498 intermittent soil drying sustain grain yield of field grown wheat, *F. Crop. Res.*, 62, 35–52, [https://doi.org/10.1016/S0378-](https://doi.org/10.1016/S0378-4290(99)00003-9)
499 [4290\(99\)00003-9](https://doi.org/10.1016/S0378-4290(99)00003-9), 1999.
- 500 [Amnuaylojaroen, T., Macatangay, R. C., Khodmanee, S.: Modeling the effect of VOCs from biomass burning emissions on](https://doi.org/10.1016/j.heliyon.2019.e02661)
501 [ozone pollution in upper Southeast Asia. *Heliyon*. 2019 Oct 17, 5\(10\):e02661, <https://doi.org/10.1016/j.heliyon.2019.e02661>.](https://doi.org/10.1016/j.heliyon.2019.e02661)
- 502 Broberg, M. C., Hayes, F., Harmens, H., Uddling, J., Mills, G., and Pleijel, H.: Effects of ozone, drought and heat stress on
503 wheat yield and grain quality, *Agric. Ecosyst. Environ.*, 352, <https://doi.org/10.1016/j.agee.2023.108505>, 2023.
- 504 Büker, P., Morrissey, T., Briolat, A., Falk, R., Simpson, D., Tuovinen, J. P., Alonso, R., Barth, S., Baumgarten, M., Grulke,
505 N., Karlsson, P. E., King, J., Lagergren, F., Matyssek, R., Nunn, A., Ogaya, R., Pêuelas, J., Rhea, L., Schaub, M., Uddling, J.,
506 Werner, W., and Emberson, L. D.: DO3SE modelling of soil moisture to determine ozone flux to forest trees, *Atmos. Chem.*
507 *Phys.*, 12, 5537–5562, <https://doi.org/10.5194/acp-12-5537-2012>, 2012.
- 508 Chandna, P., Hodson, D. P., Singh, U. P., Singh, A. N., Gosain, A. K., Sahoo, R. N., and Gupta, R. K.: Increasing the
509 Productivity of Underutilized Lands by Targeting Resource Conserving Technologies-A GIS/Remote Sensing Approach: A
510 Case Study of Ballia District, Uttar Pradesh, in the Eastern Gangetic Plains, 43 pp., 2004.
- 511 CLRTAP: Chapter 3: Mapping critical levels for vegetation, in: Manual on methodologies and criteria for modelling and
512 mapping critical loads and levels and air pollution effects, risks and trends, 2017.
- 513 Conway, T.J., n.d.. Global mean growth rates. [online] viewed 8 February 2020, available at:
514 <https://data.giss.nasa.gov/modelforce/ghgases/fig1A.ext.txt>.
- 515 Cooper, O. R., Parrish, D. D., Ziemke, J., Balashov, N. V., Cupeiro, M., Galbally, I. E., Gilge, S., Horowitz, L., Jensen, N. R.,
516 Lamarque, J. F., Naik, V., Oltmans, S. J., Schwab, J., Shindell, D. T., Thompson, A. M., Thouret, V., Wang, Y., and Zbinden,
517 R. M.: Tropospheric Ozone Assessment Report: Global distribution and trends of tropospheric ozone: An observation-based
518 review, *Elem. Sci. Anthr.*, 2, 1–28, <https://doi.org/10.12952/journal.elementa.000029>, 2014.
- 519 Daloz, A. S., Rydsaa, J. H., Hodnebrog, Sillmann, J., van Oort, B., Mohr, C. W., Agrawal, M., Emberson, L., Stordal, F., and
520 Zhang, T.: Direct and indirect impacts of climate change on wheat yield in the Indo-Gangetic plain in India, *J. Agric. Food*
521 *Res.*, 4, 100132, <https://doi.org/10.1016/j.jafr.2021.100132>, 2021.
- 522 Doorenbos, J. and Kassam, A. H.: Crop yield response to water, *FAO Irrig. Drain. Pap.* no. 33, 33, 1979.

Earth System Science Organisation, Ministry of Earth Sciences, Indian Meteorological Department, and Climate Research and Services: Statement on climate of India during 2018, 2019.

Emberson, L. D., Ashmore, M. R., Cambridge, H. M., Simpson, D., and Tuovinen, J. : Modelling stomatal ozone flux across Europe, *Environ. Pollut.*, 109, 403–413, 2000a.

Emberson, L. D., Simpson, D., Tuovinen, J., Ashmore, M. R., and Cambridge, H. M.: Towards a model of ozone deposition and stomatal uptake over Europe, in: Research Note No. 42, EMEP/MSC-W 6/2000, 2000b.

Emberson, L. D., Pleijel, H., Ainsworth, E. A., van den Berg, M., Ren, W., Osborne, S., Mills, G., Pandey, D., Dentener, F., B  ker, P., Ewert, F., Koeble, R., and Van Dingenen, R.: Ozone effects on crops and consideration in crop models, *Eur. J. Agron.*, 100, 19–34, <https://doi.org/10.1016/j.eja.2018.06.002>, 2018.

[Emmerichs, T., Al Mamun, A., Emberson, L., Mao, H., Zhang, L., Ran, L., Betancourt, C., Wong, A., Koren, G., Gerosa, G., Huang, M., and Guaita, P.: Can atmospheric chemistry deposition schemes reliably simulate stomatal ozone flux across global land covers and climates?, *EGUsphere* \[preprint\], <https://doi.org/10.5194/egusphere-2025-429>, 2025.](#)

Fangmeier, A., B  ckerhoff, U., Gr  ters, U., and J  ger, H. J.: Growth and yield responses of spring wheat (*Triticum aestivum* L. CV. Turbo) grown in open-top chambers to ozone and water stress, *Environ. Pollut.*, 83, 317–325, [https://doi.org/10.1016/0269-7491\(94\)90153-8](https://doi.org/10.1016/0269-7491(94)90153-8), 1994.

Farooq, M., Hussain, M., and Siddique, K. H. M.: Drought Stress in Wheat during Flowering and Grain-filling Periods, *CRC. Crit. Rev. Plant Sci.*, 33, 331–349, <https://doi.org/10.1080/07352689.2014.875291>, 2014.

Feng, Z., Kobayashi, K., and Ainsworth, E. A.: Impact of elevated ozone concentration on growth, physiology, and yield of wheat (*Triticum aestivum* L.): A meta-analysis, *Glob. Chang. Biol.*, 14, 2696–2708, <https://doi.org/10.1111/j.1365-2486.2008.01673.x>, 2008.

Feng, Z., Wang, L., Pleijel, H., Zhu, J., and Kobayashi, K.: Differential effects of ozone on photosynthesis of winter wheat among cultivars depend on antioxidative enzymes rather than stomatal conductance, *Sci. Total Environ.*, 572, 404–411, <https://doi.org/10.1016/j.scitotenv.2016.08.083>, 2016.

Fischer, G., Tubiello, F. N., van Velthuisen, H., and Wiberg, D. A.: Climate change impacts on irrigation water requirements: Effects of mitigation, 1990–2080, *Technol. Forecast. Soc. Change*, 74, 1083–1107, <https://doi.org/10.1016/j.techfore.2006.05.021>, 2007.

Fishman, R.: Groundwater depletion limits the scope for adaptation to increased rainfall variability in India, *Clim. Change*, 147, 195–209, <https://doi.org/10.1007/s10584-018-2146-x>, 2018.

Fowler, D., Amann, M., Anderson, R., Ashmore, M., Cox, P., Depledge, M., Derwent, D., Grennfelt, P., Hewitt, N., Hov, O., Jenkin, M., Kelly, F., Liss, P., Pilling, M., Pyle, J., Slingo, J., and Stevenson, D.: Ground-level ozone in the 21st century: future trends, impacts and policy implications, 134 pp., 2008.

Fu, T. M. and Tian, H.: Climate Change Penalty to Ozone Air Quality: Review of Current Understandings and Knowledge Gaps, *Curr. Pollut. Reports*, 5, 159–171, <https://doi.org/10.1007/s40726-019-00115-6>, 2019.

556 Gelang, J., Pleijel, H., Sild, E., Danielsson, H., Younis, S., and Selldén, G.: Rate and duration of grain filling in relation to flag
 557 leaf senescence and grain yield in spring wheat (*Triticum aestivum*) exposed to different concentrations of ozone, *Physiol.*
 558 *Plant.*, 110, 366–375, <https://doi.org/10.1111/j.1399-3054.2000.1100311.x>, 2000.
 559 Gent, P. R., Danabasoglu, G., Donner, L. J., Holland, M. M., Hunke, E. C., Jayne, S. R., Lawrence, D. M., Neale, R. B., Rasch,
 560 P. J., Vertenstein, M., Worley, P. H., Yang, Z. L., and Zhang, M.: The community climate system model version 4, *J. Clim.*,
 561 24, 4973–4991, <https://doi.org/10.1175/2011JCLI4083.1>, 2011.
 562 Ghosh, A., Agrawal, M., and Agrawal, S. B.: Effect of water deficit stress on an Indian wheat cultivar (*Triticum aestivum* L.
 563 HD 2967) under ambient and elevated level of ozone, *Sci. Total Environ.*, 714, 136837,
 564 <https://doi.org/10.1016/j.scitotenv.2020.136837>, 2020.
 565 Ghude, S. D., Jena, C., Chate, D. M., Beig, G., Pfister, G. G., Kumar, R., and Ramanathan, V.: Reductions in India’s crop yield
 566 due to ozone, *Geophys. Res. Lett.*, 41, 5685–5691, <https://doi.org/10.1002/2014GL060930>, 2014.
 567 Grell, G. A., Peckham, S. E., Schmitz, R., McKeen, S. A., Frost, G., Skamarock, W. C., and Eder, B.: Fully coupled “online”
 568 chemistry within the WRF model, *Atmos. Environ.*, 39, 6957–6975, <https://doi.org/10.1016/j.atmosenv.2005.04.027>, 2005.
 569 Harmens, H., Hayes, F., Sharps, K., Radbourne, A., and Mills, G.: Can reduced irrigation mitigate ozone impacts on an ozone-
 570 sensitive african wheat variety?, *Plants*, 8, <https://doi.org/10.3390/plants8070220>, 2019.
 571 Haworth, M., Marino, G., Loreto, F., and Centritto, M.: Integrating stomatal physiology and morphology: evolution of stomatal
 572 control and development of future crops, *Oecologia*, 197, 867–883, <https://doi.org/10.1007/s00442-021-04857-3>, 2021.
 573 He, C. and Zhou, T.: Responses of the western North Pacific subtropical high to global warming under RCP4.5 and RCP8.5
 574 scenarios projected by 33 CMIP5 models: The dominance of tropical Indian Ocean-tropical western Pacific SST gradient, *J.*
 575 *Clim.*, 28, 365–380, <https://doi.org/10.1175/JCLI-D-13-00494.1>, 2015.
 576 Hodnebrog, O., Marelle, L., Alterskjær, K., Wood, R. R., Ludwig, R., Fischer, E. M., Richardson, T. B., Forster, P. M.,
 577 Sillmann, J., and Myhre, G.: Intensification of summer precipitation with shorter time-scales in Europe, *Environ. Res. Lett.*,
 578 14, <https://doi.org/10.1088/1748-9326/ab549c>, 2019.
 579 Houshmandfar, A., Fitzgerald, G. J., O’Leary, G., Tausz-Posch, S., Fletcher, A., and Tausz, M.: The relationship between
 580 transpiration and nutrient uptake in wheat changes under elevated atmospheric CO₂, *Physiol. Plant.*, 163, 516–529,
 581 <https://doi.org/10.1111/pp1.12676>, 2018.
 582 Jain, M., Singh, B., Srivastava, A. A. K., Malik, R. K., McDonald, A. J., and Lobell, D. B.: Using satellite data to identify the
 583 causes of and potential solutions for yield gaps in India’s Wheat Belt, *Environ. Res. Lett.*, 12, [https://doi.org/10.1088/1748-](https://doi.org/10.1088/1748-9326/aa8228)
 584 [9326/aa8228](https://doi.org/10.1088/1748-9326/aa8228), 2017.
 585 Jain, V., Tripathi, N., Tripathi, S. N., Gupta, M., Sahu, L. K., Murari, V., Gaddamidi, S., Shukla, A. K., and Prevot, A. S. H.:
 586 Real-time measurements of non-methane volatile organic compounds in the central Indo-Gangetic basin, Lucknow, India:
 587 source characterisation and their role in O₃ and secondary organic aerosol formation, *Atmos. Chem. Phys.*, 23, 3383–3408,
 588 <https://doi.org/10.5194/acp-23-3383-2023>, 2023.

589 Joshi, A. K., Chand, R., Arun, B., Singh, R. P., and Ortiz, R.: Breeding crops for reduced-tillage management in the intensive,
590 rice-wheat systems of South Asia, *Euphytica*, 153, 135–151, <https://doi.org/10.1007/s10681-006-9249-6>, 2007.

591 Jumin, E., Zaini, N., Ahmed, A. N., Abdullah, S., Ismail, M., Sherif, M., Sefelnasr, A., and El-Shafie, A.: Machine learning
592 versus linear regression modelling approach for accurate ozone concentrations prediction, *Eng. Appl. Comput. Fluid Mech.*,
593 14, 713–725, <https://doi.org/10.1080/19942060.2020.1758792>, 2020.

594 Kangasjärvi, J., Jaspers, P., and Kollist, H.: Signalling and cell death in ozone-exposed plants, *Plant, Cell Environ.*, 28, 1021–
595 1036, <https://doi.org/10.1111/j.1365-3040.2005.01325.x>, 2005.

596 Khan, S. and Soja, G.: Yield responses of wheat to zone exposure as modified by drought-induced differences in ozone uptake,
597 *Water. Air. Soil Pollut.*, 147, 299–315, <https://doi.org/10.1023/A:1024577429129>, 2003.

598 Kumar, S. N., Aggarwal, P. K., Swaroopa Rani, D. N., Saxena, R., Chauhan, N., and Jain, S.: Vulnerability of wheat production
599 to climate change in India, *Clim. Res.*, 59, 173–187, <https://doi.org/10.3354/cr01212>, 2014.

600 Lamarque, J. F., Bond, T. C., Eyring, V., Granier, C., Heil, A., Klimont, Z., Lee, D., Lioussé, C., Mieville, A., Owen, B.,
601 Schultz, M. G., Shindell, D., Smith, S. J., Stehfest, E., Van Aardenne, J., Cooper, O. R., Kainuma, M., Mahowald, N.,
602 McConnell, J. R., Naik, V., Riahi, K., and Van Vuuren, D. P.: Historical (1850–2000) gridded anthropogenic and biomass
603 burning emissions of reactive gases and aerosols: Methodology and application, *Atmos. Chem. Phys.*, 10, 7017–7039,
604 <https://doi.org/10.5194/acp-10-7017-2010>, 2010.

605 Lamarque, J. F., Kyle, P. P., Meinshausen, M., Riahi, K., Smith, S. J., van Vuuren, D. P., Conley, A. J., and Vitt, F.: Global
606 and regional evolution of short-lived radiatively-active gases and aerosols in the Representative Concentration Pathways, *Clim.*
607 *Change*, 109, 191–212, <https://doi.org/10.1007/s10584-011-0155-0>, 2011.

608 Lobell, D. B., Ortiz-Monasterio, J. I., Sibley, A. M., and Sohu, V. S.: Satellite detection of earlier wheat sowing in India and
609 implications for yield trends, *Agric. Syst.*, 115, 137–143, <https://doi.org/10.1016/j.agsy.2012.09.003>, 2013.

610 McDonald, A. J., Balwinder-Singh, Keil, A., Srivastava, A., Craufurd, P., Kishore, A., Kumar, V., Paudel, G., Singh, S., Singh,
611 A. K., Sohane, R. K., and Malik, R. K.: Time management governs climate resilience and productivity in the coupled rice–
612 wheat cropping systems of eastern India, *Nat. Food*, 3, 542–551, <https://doi.org/10.1038/s43016-022-00549-0>, 2022.

613 Meinshausen, M., Smith, S. J., Calvin, K., Daniel, J. S., Kainuma, M. L. T., Lamarque, J., Matsumoto, K., Montzka, S. A.,
614 Raper, S. C. B., Riahi, K., Thomson, A., Velders, G. J. M., and van Vuuren, D. P. P.: The RCP greenhouse gas concentrations
615 and their extensions from 1765 to 2300, *Clim. Change*, 109, 213–241, <https://doi.org/10.1007/s10584-011-0156-z>, 2011.

616 Mills, G., Sharps, K., Simpson, D., Pleijel, H., Frei, M., Burkey, K., Emberson, L., Uddling, J., Broberg, M., Feng, Z.,
617 Kobayashi, K., and Agrawal, M.: Closing the global ozone yield gap: Quantification and cobenefits for multistress tolerance,
618 *Glob. Chang. Biol.*, 24, 4869–4893, <https://doi.org/10.1111/gcb.14381>, 2018a.

619 Mills, G., Sharps, K., Simpson, D., Pleijel, H., Broberg, M., Uddling, J., Jaramillo, F., Davies, W. J., Dentener, F., Van den
620 Berg, M., Agrawal, M., Agrawal, S. B., Ainsworth, E. A., Büker, P., Emberson, L., Feng, Z., Harmens, H., Hayes, F.,
621 Kobayashi, K., Paoletti, E., and Van Dingenen, R.: Ozone pollution will compromise efforts to increase global wheat
622 production, *Glob. Chang. Biol.*, 24, 3560–3574, <https://doi.org/10.1111/gcb.14157>, 2018b.

623 Mills, G., Pleijel, H., Malley, C. S., Sinha, B., Cooper, O. R., Schultz, M. G., Neufeld, H. S., Simpson, D., Sharps, K., Feng,
624 Z., Gerosa, G., Harmens, H., Kobayashi, K., Saxena, P., Paoletti, E., Sinha, V., and Xu, X.: Tropospheric Ozone Assessment
625 Report: Present-day ozone distribution and trends relevant to human health, *Elem. Sci. Anthr.*, 6,
626 <https://doi.org/10.1525/elementa.302>, 2018.

627 Ministry of Agriculture & Farmers Welfare: Agricultural Statistics at a Glance 2021, New Delhi, 431 pp., 2022.

628 Mishra, J. S., Poonia, S. P., Kumar, R., Dubey, R., Kumar, V., Mondal, S., Dwivedi, S. K., Rao, K. K., Kumar, R., Tamta, M.,
629 Verma, M., Saurabh, K., Kumar, S., Bhatt, B. P., Malik, R. K., McDonald, A., and Bhaskar, S.: An impact of agronomic
630 practices of sustainable rice-wheat crop intensification on food security, economic adaptability, and environmental mitigation
631 across eastern Indo-Gangetic Plains, *F. Crop. Res.*, 267, 108164, <https://doi.org/10.1016/j.fcr.2021.108164>, 2021.

632 Montith, J. L.: Evaporation and environment, *Symp. Soc. Exp. Biol.*, 19, 205–234, 1965.

633 Morgan, J. M.: Osmoregulation and Water Stress in Higher Plants, *Annu. Rev. Plant Physiol.*, 35, 299–319,
634 <https://doi.org/10.1146/annurev.pp.35.060184.001503>, 1984.

635 Mukherjee, A., Wang, S. Y. S., and Promchote, P.: Examination of the climate factors that reduced wheat yield in northwest
636 India during the 2000s, *Water*, 11, 1–13, <https://doi.org/10.3390/w11020343>, 2019.

637 Nigam, R., Vyas, S. S., Bhattacharya, B. K., Oza, M. P., and Manjunath, K. R.: Retrieval of regional LAI over agricultural
638 land from an Indian geostationary satellite and its application for crop yield estimation, *J. Spat. Sci.*, 62, 103–125,
639 <https://doi.org/10.1080/14498596.2016.1220872>, 2017.

640 Ortiz-Monasterio R., J. I., Dhillon, S. S., and Fischer, R. A.: Date of sowing effects on grain yield and yield components of
641 irrigated spring wheat cultivars and relationships with radiation and temperature in Ludhiana, India, *F. Crop. Res.*, 37, 169–
642 184, [https://doi.org/10.1016/0378-4290\(94\)90096-5](https://doi.org/10.1016/0378-4290(94)90096-5), 1994.

643 Pleijel, H., Danielsson, H., Gelang, J., Sild, E., and Selldén, G.: Growth stage dependence of the grain yield response to ozone
644 in spring wheat (*Triticum aestivum* L.), *Agric. Ecosyst. Environ.*, 70, 61–68, [https://doi.org/10.1016/S0167-8809\(97\)00167-](https://doi.org/10.1016/S0167-8809(97)00167-9)
645 9, 1998.

646 Pleijel, H., Eriksen, A. B., Danielsson, H., Bondesson, N., and Selldén, G.: Differential ozone sensitivity in an old and a modern
647 Swedish wheat cultivar - Grain yield and quality, leaf chlorophyll and stomatal conductance, *Environ. Exp. Bot.*, 56, 63–71,
648 <https://doi.org/10.1016/j.envexpbot.2005.01.004>, 2006.

649 Pleijel, H., Danielsson, H., Emberson, L., Ashmore, M. R., and Mills, G.: Ozone risk assessment for agricultural crops in
650 Europe: Further development of stomatal flux and flux-response relationships for European wheat and potato, *Atmos. Environ.*,
651 41, 3022–3040, <https://doi.org/10.1016/j.atmosenv.2006.12.002>, 2007.

652 Rathore, A., Gopikrishnan, G. S., and Kuttippurath, J.: Changes in tropospheric ozone over India: Variability, long-term trends
653 and climate forcing, *Atmos. Environ.*, 309, 119959, <https://doi.org/10.1016/j.atmosenv.2023.119959>, 2023.

654 Riahi, K., Rao, S., Krey, V., Cho, C., Chirkov, V., Fischer, G., Kindermann, G., Nakicenovic, N., and Rafaj, P.: RCP 8.5-A
655 scenario of comparatively high greenhouse gas emissions, *Clim. Change*, 109, 33–57, [https://doi.org/10.1007/s10584-011-](https://doi.org/10.1007/s10584-011-0149-y)
656 0149-y, 2011.

Roy, S., Beig, G., and Jacob, D.: Seasonal distribution of ozone and its precursors over the tropical Indian region using regional chemistry-transport model, *J. Geophys. Res. Atmos.*, 113, 1–15, <https://doi.org/10.1029/2007JD009712>, 2008.

Roy, S. D., Beig, G., and Ghude, S. D.: Exposure-plant response of ambient ozone over the tropical Indian region, *Atmos. Chem. Phys.*, 9, 5253–5260, <https://doi.org/10.5194/acp-9-5253-2009>, 2009.

Ruane, A. C., Rosenzweig, C., Asseng, S., Boote, K. J., Elliott, J., Ewert, F., Jones, J. W., Martre, P., McDermid, S. P., Müller, C., Snyder, A., and Thorburn, P. J.: An AgMIP framework for improved agricultural representation in integrated assessment models, *Environ. Res. Lett.*, 12, <https://doi.org/10.1088/1748-9326/aa8da6>, 2017.

Rydsaa, J. H., Stordal, F., Gerosa, G., Finco, A., and Hodnebrog: Evaluating stomatal ozone fluxes in WRF-Chem: Comparing ozone uptake in Mediterranean ecosystems, *Atmos. Environ.*, 143, 237–248, <https://doi.org/10.1016/j.atmosenv.2016.08.057>, 2016.

[Sharma, A., Ojha, N., Pozzer, A., Mar, K. A., Beig, G., Lelieveld, J., and Gunthe, S. S.: WRF-Chem simulated surface ozone over south Asia during the pre-monsoon: effects of emission inventories and chemical mechanisms, *Atmos. Chem. Phys.*, 17, 14393–14413, <https://doi.org/10.5194/acp-17-14393-2017>, 2017](#)

Sharma, A., Ojha, N., Pozzer, A., Beig, G., and Gunthe, S. S.: Revisiting the crop yield loss in India attributable to ozone, *Atmos. Environ. X*, 1, 100008, <https://doi.org/10.1016/j.aeaoa.2019.100008>, 2019.

[Sharma, A., C. Venkataraman, K. Muduchuru, V. Singh, A. Kesarkar, S. Ghosh, and S. Dey., Aerosol radiative feedback enhances particulate pollution over India: A process understanding, *Atmos. Environ.*, 298, 119609, doi: <https://doi.org/10.1016/j.atmosenv.2023.119609>, 2023](#)

Shukla, K., Srivastava, P. K., Banerjee, T., and Aneja, V. P.: Trend and variability of atmospheric ozone over middle Indo-Gangetic Plain: impacts of seasonality and precursor gases, *Environ. Sci. Pollut. Res.*, 24, 164–179, <https://doi.org/10.1007/s11356-016-7738-2>, 2017.

Shuttleworth, W. J. and Wallace, J. S.: Evaporation from sparse crops-an energy combination theory, *Q. J. R. Meteorol. Soc.*, 111, 839–855, <https://doi.org/10.1002/qj.49711146510>, 1985.

Singh, A. A. and Agrawal, S. B.: Tropospheric ozone pollution in India: effects on crop yield and product quality, *Environ. Sci. Pollut. Res.*, 24, 4367–4382, <https://doi.org/10.1007/s11356-016-8178-8>, 2017.

Steduto, P., Hsiao, T. C., Fereres, E., and Raes, D.: Crop yield response to water, *FAO Irrigation and Drainage Paper no. 66*, 2012.

Stockwell, W. R., Middleton, P., Chang, J. S., and Tang, X.: The second generation regional acid deposition model chemical mechanism for regional air quality modeling, *J. Geophys. Res. Atmos.*, 95, 16343–16367, <https://doi.org/10.1029/JD095iD10p16343>, 1990.

Tai, A. P. K. and Martin, M. V.: Impacts of ozone air pollution and temperature extremes on crop yields: Spatial variability, adaptation and implications for future food security, *Atmos. Environ.*, 169, 11–21, <https://doi.org/10.1016/j.atmosenv.2017.09.002>, 2017.

Tai, A. P. K., Martin, M. V., and Heald, C. L.: Threat to future global food security from climate change and ozone air pollution, *Nat. Clim. Chang.*, 4, 817–821, <https://doi.org/10.1038/nclimate2317>, 2014.

Tans, P.P., Conway, T.J., n.d. Global means constructed using about 70 CMDL CCGG Sampling Network station data. [online] viewed 8 February 2020, available at: <https://data.giss.nasa.gov/modelforce/ghgases/Fig1A.ext.txt>.

Teixeira, E., Fischer, G., van Velthuizen, H., van Dingenen, R., Dentener, F., Mills, G., Walter, C., and Ewert, F.: Limited potential of crop management for mitigating surface ozone impacts on global food supply, *Atmos. Environ.*, 45, 2569–2576, <https://doi.org/10.1016/j.atmosenv.2011.02.002>, 2011.

Tripathi, A. and Mishra, A. K.: The Wheat Sector in India: Production, Policies and Food Security, in: *The Eurasian Wheat Belt and Food Security: Global and Regional Aspects*, 275–296, https://doi.org/10.1007/978-3-319-33239-0_17, 2017.

[Tuovinen, J.-P., Ashmore, M. R., Emberson, L.D. and Simpson, D.: Testing and improving the EMEP ozone deposition model, *Atmos. Environ.*, 38, 2373–2385, <https://doi.org/10.1016/j.atmosenv.2004.01.026>](#)

van Vuuren, D. P., Edmonds, J., Kainuma, M., Riahi, K., Thomson, A., Hibbard, K., Hurtt, G. C., Kram, T., Krey, V., Lamarque, J. F., Masui, T., Meinshausen, M., Nakicenovic, N., Smith, S. J., and Rose, S. K.: The representative concentration pathways: An overview, *Clim. Change*, 109, 5–31, <https://doi.org/10.1007/s10584-011-0148-z>, 2011.

UNDESA (United Nations Department of Economic and Social Affairs), 2022. *World Population Prospects 2022: Summary of Results*. UN DESA/POP/2-22/TR/NO.3.

Wada, Y., Wisser, D., Eisner, S., Flörke, M., Gerten, D., Haddeland, I., Hanasaki, N., Masaki, Y., Portmann, F. T., Stacke, T., Tessler, Z., and Schewe, J.: Multimodel projections and uncertainties of irrigation water demand under climate change, *Geophys. Res. Lett.*, 40, 4626–4632, <https://doi.org/10.1002/grl.50686>, 2013.

Wang, H. W., Li, X. B., Wang, D., Zhao, J., He, H. di, and Peng, Z. R.: Regional prediction of ground-level ozone using a hybrid sequence-to-sequence deep learning approach, *J. Clean. Prod.*, 253, 119841, <https://doi.org/10.1016/j.jclepro.2019.119841>, 2020.

[Wilkinson, S. and Davies, W.J.: Drought, ozone, ABA and ethylene: new insights from cell to plant to community, *Plant, Cell and Env.*, 33, 4, <https://doi.org/10.1111/j.1365-3040.2009.02052.x>, 2011.](#)

[Wu, S., Mickley, L. J., Leibensperger, E. M., Jacob, D. J., Rind, D., and Streets, D. G.: Effects of 2000–2050 global change on ozone air quality in the United States, *Journal of Geophysical Research: Atmospheres*, 113, D06 302, <https://doi.org/10.1029/2007JD008917>, 2008.](#)

Yadav, D. S., Rai, R., Mishra, A. K., Chaudhary, N., Mukherjee, A., Agrawal, S. B., and Agrawal, M.: ROS production and its detoxification in early and late sown cultivars of wheat under future O₃ concentration, *Sci. Total Environ.*, 659, 200–210, <https://doi.org/10.1016/j.scitotenv.2018.12.352>, 2019.

Yadav, D. S., Mishra, A. K., Rai, R., Chaudhary, N., Mukherjee, A., Agrawal, S. B., and Agrawal, M.: Responses of an old and a modern Indian wheat cultivar to future O₃ level: Physiological, yield and grain quality parameters, *Environ. Pollut.*, 259, <https://doi.org/10.1016/j.envpol.2020.113939>, 2020.

723 Yadav, D. S., Agrawal, S. B., and Agrawal, M.: Ozone flux-effect relationship for early and late sown Indian wheat cultivars:
724 Growth, biomass, and yield, *F. Crop. Res.*, 263, 108076, <https://doi.org/10.1016/j.fcr.2021.108076>, 2021.

725 Yao, A. Y. M.: Agricultural potential estimated from the ratio of actual to potential evapotranspiration, *Agric. Meteorol.*, 13,
726 405–417, [https://doi.org/10.1016/0002-1571\(74\)90081-8](https://doi.org/10.1016/0002-1571(74)90081-8), 1974.

727 [Zanis, P., Akritidis, D., Turnock, S., Naik, V., Szopa, S., Georgoulas, A.K., Bauer, S.E., Deushi, M., Horowitz, L.W., Keeble,](#)
728 [J. and Le Sager, P., 2022. Climate change penalty and benefit on surface ozone: a global perspective based on CMIP6 earth](#)
729 [system models. *Environmental Research Letters*, 17\(2\), p.024014](#)

730 Zaveri, E. and Lobell, D. B.: The role of irrigation in changing wheat yields and heat sensitivity in India, *Nat. Commun.*, 10,
731 <https://doi.org/10.1038/s41467-019-12183-9>, 2019.

732 Zaveri, E., Grogan, D. S., Fisher-Vanden, K., Frolking, S., Lammers, R. B., Wrenn, D. H., Prusevich, A., and Nicholas, R. E.:
733 Invisible water, visible impact: Groundwater use and Indian agriculture under climate change, *Environ. Res. Lett.*, 11,
734 <https://doi.org/10.1088/1748-9326/11/8/084005>, 2016.

735

736